Journal of Computational Physics **180,** 497–505 (2002)
doi:10.1006/jcph.2002.7096

Nonlinear Landau Damping in Spherically Symmetric Vlasov Poisson Systems

Claus Heerlein and Günter Zwicknagel

Institut für Theoretische Physik II, Universität Erlangen-Nürnberg, Staudtstraße 7, D-91058 Erlangen, Germany
E-mail: heerlein@physik.uni-erlangen.de

Received August 21, 2001; revised May 7, 2002

The Vlasov Poisson system is a partial differential equation widely used to describe collisionless plasma. It is formulated in a six-dimensional phase space, this prohibits a numerical solution on a complete phase space grid. In some applications, however, spherical symmetry is given, which introduces singularities into the Vlasov Poisson equation. We focus on such problems and propose a stable algorithm using accommodating boundaries. At first, the method is tested in the linear regime, where analytical solutions are available. Thereafter it is applied to large disturbances from equilibrium.

Key Words: Vlasov Poisson equation; accommodating boundaries; operator splitting; Landau damping.

1. PHYSICAL BACKGROUND

1.1. The Vlasov Poisson System

The Vlasov Poisson system is a partial integrodifferential equation describing classical one-component plasma (OCP) in the limit of weak coupling.

Let f be the phase space density as a function of the time t, the position $\mathbf{r}$, and the momentum $\mathbf{p}$. We chose as units for the inverse plasma frequency, the Debye length, and the thermal momentum

$$\omega_{\mathrm{p}}^{-1} = \sqrt{\frac{\varepsilon_0 m}{e^2 n_0}},$$

$$\lambda_{\mathrm{D}} = \sqrt{\frac{\varepsilon_0 k_{\mathrm{B}} T}{e^2 n_0}},$$

$$p_{\mathrm{th}} = m\lambda_{\mathrm{D}}\omega_{\mathrm{p}} = \sqrt{m k_{\mathrm{B}} T}.$$

The particles of the OCP may be interpreted as electrons. However we include the particle

0021-9991/02 $35.00

charge in the unit of the electric field, here given by $E_0 = -\omega_p p_{th}/e$. In these units the Vlasov Poisson system reads with a neutralizing background

$$\frac{\partial f}{\partial t} + \mathbf{p} \cdot \frac{\partial f}{\partial \mathbf{r}} + \mathbf{E}_{mf} \cdot \frac{\partial f}{\partial \mathbf{p}} = 0, \tag{1}$$

$$\nabla \cdot \mathbf{E}_{mf} = \int d^3 p f - 1. \tag{2}$$

The thermal equilibrium without an external field is the Maxwell Boltzmann distribution

$$f_0 := \frac{1}{(2\pi)^{3/2}} \exp\left(-\frac{p^2}{2}\right). \tag{3}$$

As this state is reached by collisions, it is not necessarily a convergence point of the Vlasov Poisson system; however f_0 is clearly a stationary solution. So we define a distortion f_1 through

$$f(t, \mathbf{r}, \mathbf{p}) = f_0(\mathbf{p}) + f_1(t, \mathbf{r}, \mathbf{p}), \tag{4}$$

which results in the Vlasov Poisson equation for f_1,

$$\frac{\partial f_1}{\partial t} + \mathbf{p} \cdot \frac{\partial f_1}{\partial \mathbf{r}} + \mathbf{E}_{mf} \cdot \frac{\partial f_1}{\partial \mathbf{p}} = -\mathbf{E}_{mf} \cdot \frac{\partial f_0}{\partial p}, \tag{5}$$

$$\nabla \cdot \mathbf{E}_{mf} = \int d^3 p f_1. \tag{6}$$

1.2. Boundary Conditions

For the envisioned application we use accommodating boundaries, which describe particles colliding with the boundary as instantaneously thermalized. According to a model of Maxwell a container wall can be described by a superposition of accommodation and specular reflection. And experimental investigations in dilute gases have shown that the accommodating contribution dominates [1].

We now consider an arbitrary point $\mathbf{r}$ on the boundary with the outward normal $\mathbf{n}$. With the outflow

$$j := \int\limits_{p_\perp > 0} d^3 p p_\perp f, \tag{7}$$

we demand $f = \sqrt{2\pi} j f_0$ on the inflow boundary ($p_\perp := \mathbf{n} \cdot \mathbf{p} < 0$) and thus the total mass flow vanishes:

$$\begin{aligned} \int d^3 p p_\perp f &= \int\limits_{p_\perp < 0} d^3 p p_\perp f + \int\limits_{p_\perp > 0} d^3 p p_\perp f \\ &= \sqrt{2\pi} j \int\limits_{p_\perp < 0} d^3 p p_\perp f_0 + j = 0. \end{aligned} \tag{8}$$

With the knowledge of the solution in the interior, integral (7) over the outflow region can be evaluated at each time step and so the boundary condition is well posed.

Further we have only a limited volume in momentum space. Here the boundary conditions are less crucial since the phase space density decays strongly for large p. For simplicity a zero boundary condition is chosen there.

1.3. Spherical Symmetry and Coordinate Systems

So far the full Vlasov Poisson system in $3 + 3$ dimensional phase space has been considered. However for a numerical solution this system requires an extraordinarily large grid size even in a very moderate resolution.

Luckily several interesting applications are isotropic, such as nonlinear Landau damping or transient Debye shielding. Spherical symmetry reduces the phase space under consideration to a three-dimensional manyfold since f may only depend on rotational invariants, which are the distance r from the center, the norm of the momentum p, and the scalar product $s := \mathbf{r} \cdot \mathbf{p}$.

Taking the full angular dependence into account we add a considerable challenge to numerical methods since formal singularities occur for $r = 0$ and $p = 0$. Due to these singularities a direct solution with finite differences becomes unfeasible [2]. Straightforward transformation for the Vlasov equation in coordinates r, p, and s yields

$$\frac{\partial f}{\partial t} + \frac{s}{r}\frac{\partial f}{\partial r} + E\frac{s}{rp}\frac{\partial f}{\partial p} + (p^2 + Er)\frac{\partial f}{\partial s} = 0, \tag{9}$$

while the integral transformation of the Poisson equation gives

$$\frac{dE}{dr} = \int_0^\infty \mathrm{d}p \int_\infty^\infty \mathrm{d}s\, 8\pi^2 rp\, f(r, p, s), \tag{10}$$

with the boundary condition $E(0) = 0$, due to symmetry. The integration region in (r, p, s) coordinates however is not cone shaped, which prohibits the use of finite elements [3]. It can be shown easily that transformations by arbitrary powers of r and p cannot simultaneously resolve this problem and lift the singularities [4].

The conservation of angular momentum $l = \sqrt{r^2p^2 - (\mathbf{r} \cdot \mathbf{p})^2}$ in the central force problem invites the use of this quantity as an independent variable. The coordinates (l, p, r), however, are not a suitable choice because in the $s = 0$ plane they point in coplanar directions. The problem may be fixed by taking the radial momentum $q := \mathbf{e}_r \cdot \mathbf{p}$ instead of p as an independent variable. The Vlasov equation then reads

$$\frac{\partial f}{\partial t} + q\frac{\partial f}{\partial r} + \left(\frac{l^2}{r^3} + E\right)\frac{\partial f}{\partial q} = 0. \tag{11}$$

Clearly the centrifugal barrier l^2/r^3 is singular and again the singularity cannot be lifted by introducing arbitrary powers of l, q, and r as independent variables. Finally the Poisson equation becomes

$$\frac{dE}{dr} = \int_0^\infty \mathrm{d}l \int_\infty^\infty \mathrm{d}q\, 8\pi^2 l f(l, q, r). \tag{12}$$

Eventually, a further interesting set of coordinates is motivated by the free motion. Let $\tau := \mathbf{r} \cdot \mathbf{p}/p^2$ be the distance from the plane of closest approach and $b := \sqrt{r^2 - \tau^2}$ the collision parameter. Then the field-free Vlasov equation in coordinates (l, b, τ) is simply

$$\frac{\partial f}{\partial t} + \frac{\partial f}{\partial \tau} = 0, \tag{13}$$

as then both l and b are conserved. The coefficients in the full Vlasov equation get more involved with $E \not\equiv 0$, though this case is not to be considered in the following.

2. NUMERICAL METHOD

In the previous section coordinates (l, b, τ) were constructed in which the free propagation becomes a homogeneous flow. Furthermore the action of the electric field is a sheer flow in (l, q, r) coordinates. This invites the use of an operator splitting scheme based on the pioneering work for Cartesian systems by Cheng and Knorr [5] and Shoucri and Gagne [6]. We therefore consider the free Liouville operator $\hat{L}_\tau := q\partial_r + l^2/r^3\partial_q = \partial_\tau$, and its complement $\hat{L}_q := E\partial_q$, by which the operator notation for the Vlasov equation (11) becomes

$$(\partial_t + \hat{L}) f_1 = g, \tag{14}$$

with $\hat{L} := \hat{L}_\tau + \hat{L}_q$ and $g := -Eqf_0$.

It has been shown that together with accommodating boundaries [7] $-\hat{L}_\tau$ is the infinitesimal generator of a $\mathcal{C}_0$ semigroup and $\hat{L}_q$ is bounded. Hence the homogenous solution for an initial distribution f_1^0 may be written as

$$f_1(t) = \exp(-t\hat{L}) f_1^0. \tag{15}$$

At this stage however it remains difficult to give the operator $\exp(-t\hat{L})$ explicitly. For a numerical integration with the time step Δt we use a symmetric splitting scheme

$$\exp(\Delta t \hat{L}) = \exp\left(\frac{\Delta t}{2}\hat{L}_\tau\right) \exp(\Delta t \hat{L}_q) \exp\left(\frac{\Delta t}{2}\hat{L}_\tau\right) + \mathcal{O}(\Delta t^2). \tag{16}$$

To construct the time step explicitly, we change back to a coordinate representation. With fractional time steps the backward characteristics are given by

$$\begin{aligned} f^{n+\frac{1}{3}}(l, b, \tau) &= f^n\left(l, b, \tau - \frac{\Delta t}{2}\right), \\ f^{n+\frac{2}{3}}(l, q, r) &= f^{n+\frac{1}{3}}(l, q - E\Delta t, r), \\ f^{n+1}(l, b, \tau) &= f^{n+\frac{2}{3}}\left(l, b, \tau - \frac{\Delta t}{2}\right). \end{aligned} \tag{17}$$

Numerical evaluation of this scheme needs the coordinate transformations

$$\begin{aligned} b(l,q,r) &= \frac{lr}{\sqrt{l^2+q^2r^2}}, \quad & q(l,b,\tau) &= \frac{l^2\tau}{b_2\sqrt{l^2\tau^2+b^4}}, \\ \tau(l,q,r) &= \frac{qr^3}{l^2+q^2r^2}, & r(l,b,\tau) &= \frac{\sqrt{l^2\tau^2+b^4}}{b}. \end{aligned} \tag{18}$$

As the Poisson equation (12) is formulated in r, we prefer an equidistant grid in (l, q, r) coordinates to represent f_1 in each time step. The characteristics of the problem are given by (17) and (18) and generally require the evaluation of f_1 between the grid points. We are using cubic interpolation and the application shows that charge conservation is fulfilled to a fair amount of less than 10^{-5} times the initial disturbance. The Poisson equation is simply solved by integration of Gauss's law. The implementation of our algorithm scales well on parallel architectures. This is a consequence of the parallelization in angular momentum slices, which are coupled just by the mean field and thus need little interprocess communication.

3. APPLICATION

Now the proposed algorithm is to be tested in a physical application which allows a comparison of the simulation with analytic results. We impose an initial density disturbance and study its evolution. Therefore we assume that the initial disturbance is spherically symmetric and consists of pure Fourier modes only. This requires the initial spatial density to be a spherical Bessel function of order zero:

$$n_1(t=0) = \alpha j_0(kr). \tag{19}$$

Additionally, charge neutrality in the simulation box of radius R requires discrete values for the wave number k, with

$$j_1(kR) = 0 \Leftrightarrow \tan(kR) = kR, \tag{20}$$

for which the total charge

$$Q_1 = \int_0^R \mathrm{d}r\, 4\pi r^2 n_1(t=0,r) = \frac{4\pi R^2\alpha}{k} j_1(kR) \tag{21}$$

vanishes. We further impose a homogenous temperature and initialize the phase space density as

$$f_1(t=0) = n_1(t=0) f^0. \tag{22}$$

In the following test run we have chosen a grid volume of $R = 33.95\,\lambda_\mathrm{D}$ and $P = 6.0\,p_\mathrm{th}$. This reduces the influence of the momentum boundary to a considerably small effect due to the initial phase space density reduced by a factor of $\exp(-\frac{1}{2}P^2) < 10^{-8}$ at the boundary. At first we focus on the mode $k = 0.6\,\lambda_\mathrm{D}^{-1}$, for which linear theory gives an oscillation frequency $\omega_0 = 1.546\ \omega_\mathrm{p}$ and a damping rate $\gamma_0 = 0.2642\ \omega_\mathrm{p}$. Thus a phase

velocity is $v_{\rm ph} = 2.57 v_{\rm th}$ and resonant particle trajectories are well inside the simulation volume. Further, all numerical calculations shown are done with a time step of $\Delta t = 0.1\omega_{\rm p}^{-1}$ and a resolution of $\Delta r = 0.1\,\lambda_{\rm D}$, $\Delta q = 0.1\,p_{\rm th}$, $\Delta l = 0.1\,P\lambda_{\rm D} p_{\rm th}$. Further refinement does not alter the physical results significantly.

The proposed numerical method is applicable for arbitrary deviations from equilibrium. Our first intention is now to validate the code in comparison to analytical theories describing the linear approximation, i.e., the linear Vlasov equation wherein the term Ef_1 is neglected. The related theory of Landau damping is strictly linear; however it holds as an approximative solution for some period after initialization [8]. For an initial amplitude α of the disturbance, Landau damping is a good approximation for times t below the bounce time $\tau = (\alpha\lambda_{\rm D}^3)^{-1/2}\omega_{\rm p}^{-1}$. For the test at issue $\alpha = 10^{-5}\lambda_{\rm D}^{-3}$ was chosen to suppress the nonlinearities and thus $\tau = 316\,\omega_{\rm p}^{-1}$.

A first test for the correctness of the numerical method is given by charge conservation. In Fig. 1 the evolution of the mean charge density is shown. The observed oscillation corresponds to the plasma oscillation and the overall loss of charge is an effect of numerical damping. The maximum violation of charge neutrality stays below 0.0002 during the simulation time. Additionally the relative entropy $S_{\rm rel} = (S(t) - S(0))/S(0)$ of the disturbance is shown with

$$S = \int_0^L {\rm d}l \int_{-P}^{P} {\rm d}q \int_0^{R_0} {\rm d}r\, 8\pi^2 l f \ln f. \tag{23}$$

Obviously the entropy is a constant of the Vlasov Poisson equation. However in our simulation we have additional effects from the boundaries, which are responsible for the superposed oscillation. It is reassuring in respect to the influence of the boundary and numerical errors that the values of $S_{\rm rel}^1$ stay rather small.

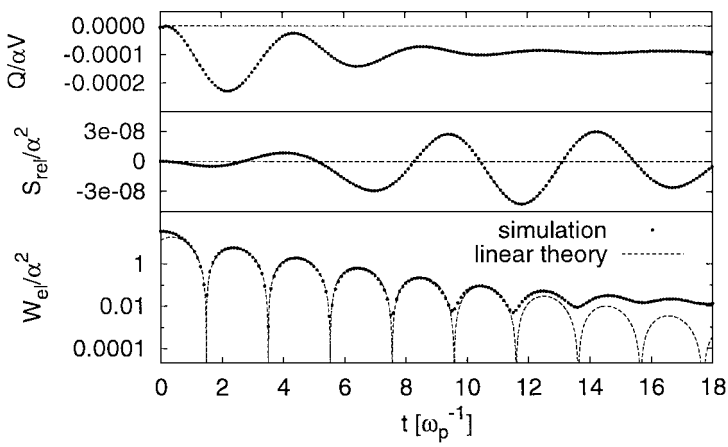

FIG. 1. Linear plasma oscillation in the mode $k = 0.6\,\lambda_{\rm D}^{-1}$ over $18\,\omega_{\rm p}^{-1}$. (Top panel) Charge density; (central panel) entropy of disturbance; (bottom panel) electrical energy in control volume. All quantities are in plasma units, α is the amplitude of the initial disturbance (19), and V is the simulation volume. The linear theory yields $\omega_0 = 1.546\,\omega_{\rm p}$ and $\gamma_0 = 0.02642\,\omega_{\rm p}$ in this case, and amplitude and phase are adopted to the numerical results. Simulation parameters: $\alpha = 10^{-5}\,\lambda_{\rm D}^{-3}$, $R = 33.95\,\lambda_{\rm D}$, $P = 6.0\,p_{\rm th}$, $\Delta t = 0.1\,\omega_{\rm p}^{-1}$, $\Delta r = 0.1\,\lambda_{\rm D}$, $\Delta q = 0.1\,p_{\rm th}$, $\Delta l = 0.1 P\,\lambda_{\rm D} p_{\rm th}$.

An appropriate observable for the plasma oscillation is the total electrical field energy

$$W_{\mathrm{el}} = \frac{1}{2} \int_0^{R_0} \mathrm{d}r \, 4\pi r^2 E^2(r) \tag{24}$$

in a test volume of radius R_0, which contains the inner three nodes of the disturbance.

Eventually, Fig. 1 displays numerical results for W_{el} as a function of time and analytical results [9] for comparison. The prominent discrepancy for $t \leq 0.7\,\omega_{\mathrm{p}}^{-1}$ reflects an initial transient period, during which additionally modes with stronger damping decay. These additional modes are not taken into account for the analytic results, but are contained in the numerical calculations. For times larger than $R/v_{\mathrm{ph}} = 13.2\,\omega_{\mathrm{p}}^{-1}$ the plasma wave has propagated through the simulation volume and thus the boundary conditions yield a deviation from linear theory.

We now investigate the nonlinearities in the decay of an initial density disturbance. Therefore we regard a j_0 disturbance as above in a box of $R = 6.484\pi/k$ for various wavelengths k and amplitudes α. Observed is the normalized electrical energy $\tilde{W}_{\mathrm{el}} = W_{\mathrm{el}}/\alpha^2$ within a control volume of $R_0 = 3.471\pi/k$. The chosen box sizes are sufficient that the first few maxima of $\tilde{W}_{\mathrm{el}}$ may be observed within good numerical accuracy and without considerable influence of the boundary conditions.

Figure 2 shows time resolved calculations for $k = 0.6\,\lambda_{\mathrm{D}}^{-1}$ and $k = 1.4\,\lambda_{\mathrm{D}}^{-1}$ over the maximum range of amplitudes $\alpha = (-1, 10^{-5}, 1, 4.6)\,\lambda_{\mathrm{D}}^{-3}$. The oscillation of W_{el} is substantially altered for larger amplitudes, which becomes most clear in the first maximum at time $t^1(k)$. This allows consolidation of the information by introducing to a heuristic measure

$$\delta(k, \alpha) := \frac{1}{t^1}\left(1 - \frac{\tilde{W}_{\mathrm{el}}(t^1, k, \alpha)}{\tilde{W}_{\mathrm{el}}(t^1, k, 0)}\right) \tag{25}$$

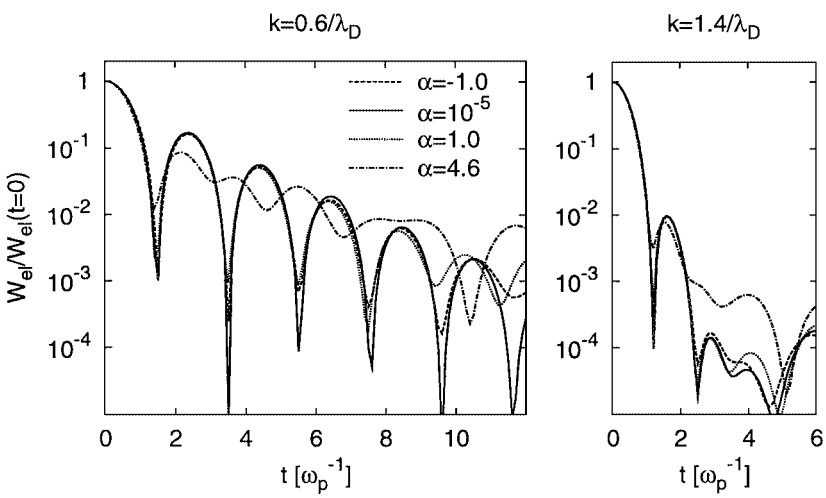

FIG. 2. Nonlinear plasma oscillation in the scaled electrical energy $\tilde{W}_{\mathrm{el}}$ for $k = 0.6\,\lambda_{\mathrm{D}}^{-1}$ (left panel) and $k = 1.4\,\lambda_{\mathrm{D}}^{-1}$ (right panel). In each array the amplitude is varied in the maximum accessible range $\alpha = -1.0\,\lambda_{\mathrm{D}}^{-3}$ (dashed), $\alpha = 10^{-5}\,\lambda_{\mathrm{D}}^{-3}$ (solid), $\alpha = 1.0\,\lambda_{\mathrm{D}}^{-3}$ (dotted), $\alpha = 4.6\,\lambda_{\mathrm{D}}^{-3}$ (dash–dotted). Numerical parameters as in Fig. 1.

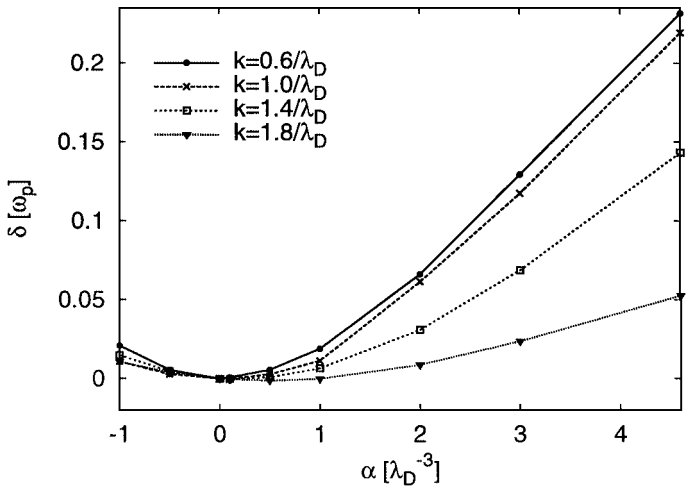

FIG. 3. The quantity δ from (25) measures the strength of nonlinear effects after the first half-oscillation. The sensitivity of the system to nonlinearities depends on the wave number k of the disturbance. Numerical parameters as in Fig. 1.

of the nonlinearities. The rate δ is plotted in Fig. 3 and gives the relative excess damping rate due to nonlinearities.

To study the influence of nonlinearities at moderate amplitudes we fit a function of the type $(A\cos(\omega t-\phi_0)\exp(-\Delta\gamma t))^2$ to $\tilde{W}_{\rm el}\exp(\gamma_0 t)$, with A,ω,ϕ, and $\Delta\gamma$ as free parameters and γ_0 as the linear damping rate. The weighting with the damping rate γ_0 guarantees that all data points in the selected time window contribute equally to the fit. The time window itself was chosen such that the higher plasma modes have already decayed and that three half-oscillation are covered. Figure 4 displays the fitted values for ω and $\gamma=\gamma_0+\Delta\gamma$ exemplarily for $k=0.6\,\lambda_{\rm D}^{-1}$. It turns out that the nonlinearities impose additional damping on the system. Further, with larger amplitude α the oscillation is detuned toward increased frequencies. For initial amplitudes higher than $\alpha=2.0\,\lambda_{\rm D}^{-3}$ the appearance of $W_{\rm el}$ is too dissimilar to a damped oscillation to perform the above fit with meaningful result.

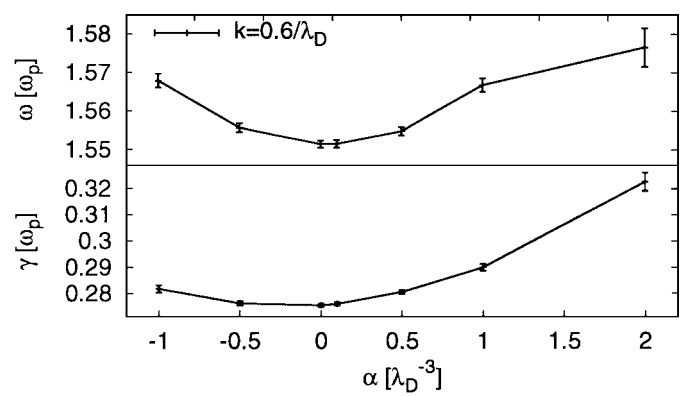

FIG. 4. In an appropriate time window a damped oscillation is fitted to the numerical results of $W_{\rm el}$. The top panel shows the best fitting oscillation frequency and the bottom the damping rate. Numerical parameters as in Fig. 1.

4. CONCLUSION

We have presented a stable numerical method for solving the Vlasov Poisson system in spherical symmetry, which can be implemented efficiently on parallel computers. The accommodating boundary condition provides enhanced robustness of the method. For large box sizes the numerical results of Landau damping are in agreement with linear theory.

The method presented here opens a wide field of physical problems to be investigated. Such are, for example, the transient density enhancement around an external ion in an electron plasma. This is an active field of research, where current experiments can be explained by models [11] to some extent; however calculations from first principles are still to be done. The method can be easily extended to cylindrical symmetry by adding two Cartesian phase space variables. This allows application in the field of the energy loss of ions in a plasma [10] and recombination.

ACKNOWLEDGMENTS

This work has been supported by the Gesellschaft für Schwerionenforschung (GSI-ER T0-2), and the John von Neumann Institute for Computing in Jülich. We are indebted C. Toepffer, P.-G. Reinhard, and C. Deutsch for their constructive comments. Also we thank G. Wellein for his contribution in parallelizing the algorithm.

REFERENCES

1. S. Harris, *An Introduction to the Theory of the Boltzmann Equation* (Holt, Rinehart & Winston, Yew York, 1971).
2. T. S. Gherega, *Numerische Simulation von räumlich eindimensionalen und zweidimensionalen Plasmen mittels finiter Differenzen*, Ph.D. thesis (Univ. Erlangen, 1997).
3. D. Braess, *Finite Elemente* (Springer-Verlag, Berlin, 1991).
4. C. Heerlein, *Numerische Analyse radialsymmetrischer Vlasov-Poisson-Systeme*, Diploma thesis (Univ. Erlangen, 1999).
5. C. Z. Cheng and G. Knorr, The integration of the Vlasov equation in configuration space, *J. Comput. Phys.* **22**, 330 (1976).
6. M. M. Shoucri and R. R. J. Gagne, Splitting schemes for the numerical solution of a two-dimensional Vlasov equation, *J. Comput. Phys.* **27**, 315 (1978).
7. C. Heerlein, *Halbgruppeneigenschaften linearisierter Vlasov-Poisson-Systeme mit akkommodierenden Randbedingungen*, Diploma thesis. (Univ. Erlangen, 1999).
8. G. Manfredi, Long time behavior of nonlinear Landau damping, *Phys. Rev. Lett.* **79**, 2815 (1997).
9. C. Seele, G. Zwicknagel, C. Toepffer, and P.-G. Reinhard, Time-dependent stopping power and influence of an infinite magnetic field, *Phys. Rev. E* **57**, 3368 (1998).
10. G. Zwicknagel, C. Toepffer, and P.-G. Reinhard, Stopping of heavy ions in plasmas at strong coupling, *Phys. Rep.* **309**, 117 (1999).
11. Q. Spreiter and C. Toepffer, A screening model for density enhancement near ions at rest in magnetized electron plasmas, *J. Phys. B* **33**, 2347 (2000).